

The Measurement of Wetting Angle by Applying an ADSA Model of Sessile Drop on Selected Textile Surfaces

Technical University of Łódź,
Computer Engineering Department,
ul. Żeromskiego 116, 90-543 Łódź, Poland
e-mail: jgoslaw@kis.p.lodz.pl

*Department of Fibre Physics
and Textile Metrology,
e-mail: wurbando@p.lodz.pl

Abstract

This paper presents a method of liquid-solid contact (wetting) angle measurement for selected textile surfaces, assuming the angles to be less than 90°. The method uses a special apparatus for acquisition of sessile drop images. Specialised image processing methods involving edge filtering, image morphology and a prior knowledge of the drop boundary location are used to extract droplet edges and the bottom line of a solid textile surface. Then ADSA profile optimisation is applied to find the liquid contact angle with respect to the bottom line. The ADSA trajectory is fitted to the drop edge data using a trust – region, non-linear optimisation algorithm, with a proposed definition of distance error measurement. The image processing and analysis methods mentioned above are implemented in a MATLAB 7.0 environment; the results of individual measurements are shown in MATLAB windows as well.

Key words: ADSA model, sessile drop, wetting angle, contact angle, capillary constant, edge detection, dilation.

as well as during the refining of products (such as printing, gluing, making apprets in liquid phase, lamination) and also when producing good mechanically resistant composite materials [3, 4].

Among the many methods of contact angle measurement, the sessile drop method [5] is noteworthy. It analyses the meniscus shape of a liquid drop put on the flat surface to be examined. The use of a small amount of liquid to investigate the surface, and the possibility of observing the kinetic phenomenon of wetting in its local zones, is an unquestionable advantage of the sessile drop method. This effect is impossible to achieve using the Wilhelmy method [5] or wicking method [6], where the end measurement result applies to the whole sample perimeter. The basic uncertainties of contact angle evaluation in the sessile drop method are the precision of the base (bottom) line location, identification of the liquid-solid-air con-

tact point and the assignment of the drop profile tangent at this point. Neumann [7, 8] replaced the procedure of subjectively setting the tangent and reading the contact angle with an ADSA numerical model (Axisymmetric Drop Shape Analysis). Since then, it has been possible to carry out angle measurement automatically with a small margin of error - ca. 0.1°. This margin of uncertainty is specific for smooth, planar and homogeneous surfaces – in such cases where the contact line of the drop with respect to a bottom solid surface is precise and easily visible.

Textile surfaces are rough to a degree; depending on the structure of the interlace of yarn strands, the fibres infill and their arrangement in the product (woven fabrics, knitted products and needled nonwoven). The application of the ADSA model for such surfaces requires a specific approach as far as setting the base line is concerned: textile surface - the liquid

Introduction

The behaviour of liquids in contact with solid surfaces can be different. Some liquids spread over surfaces making a film, whereas others wet them to a limited extent, creating drops at a given contact angle.

That contact angle between a liquid and a solid surface is a sensitive indicator of changes in the level of surface energy and changes in the chemical and supermolecular structure of the surfaces to be modified [1]. Knowledge of the contact angle enables estimation of the type of interaction between surfaces and liquids (dispersive and polar interactions) [2] and has a wide range of practical applications. It helps to predict the course of reaction during the chemical processing of surfaces in a liquid environment (washing, dyeing),

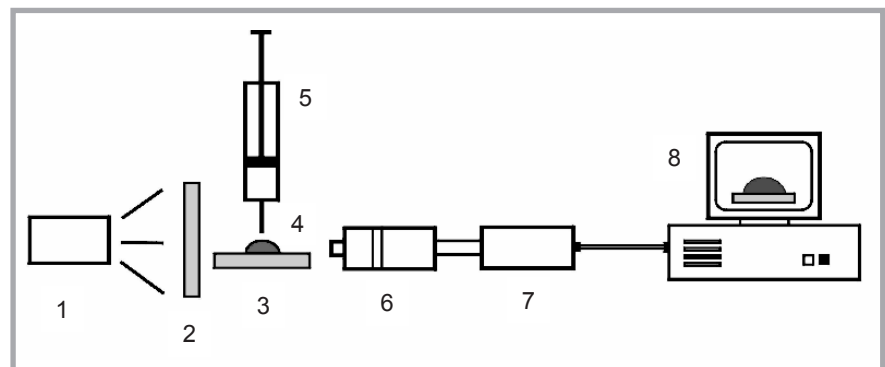


Figure 1. A block diagram of an apparatus for measuring textile wettability. 1 - light source, 2 - diffuser, 3 - measuring table, 4 - liquid droplet, 5 - manual syringe, 6 - camera lenses, 7 - CCD camera, 8 - PC computer with an image acquisition card and image processing applications.

drop, establishing the contact point of the three-phases on the base line and differentiating artefacts on the meniscus of the liquid drop. Because of this many existing commercial solutions of goniometers [9, 10] are not applicable in this case.

In this series of articles, both the numerical procedures, made for real cases of textile surfaces, and the procedures which would enable the identification of the base line and the automatic measurement of the contact angle will be presented. Light absorbing, reflecting, liquid moistened, and non-moistened surfaces will be taken into account, as well as surfaces with single protruding fibres, taking the role of artefacts on the meniscus of the liquid drop.

■ The measurement apparatus

The apparatus used for sessile drop imaging and measurement, consisting of hardware components, is shown in Figure 1. A flat textile specimen is placed on a horizontal measuring table (3). A dose of liquid (1 μ l) is injected into a textile surface by a manually driven syringe (5) creating a sessile droplet (4). The droplet (4) is illuminated by a source of visible light (1) through a diffuser plate (2), which is seen by a CCD camera (7) equipped with an appropriate set of lenses (6).

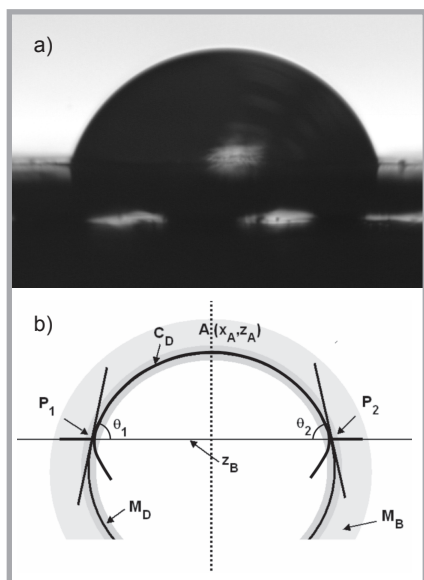


Figure 2. a) Water droplet image on an examined polyester textile. b) Droplet model showing the possible behaviour of edges (boundaries) in the background contact zone. A –the drop apex, C_D –the droplet edge, z_B –the bottom line, M_B –the mask for bottom line location, M_D –the mask of boundary data, θ_1 , θ_2 –wetting (contact) angles between textile background and liquid phase

The droplet image acquired by the camera in PAL standard (768 \times 576 pixels) is transmitted by means of a frame-grabber into a computer's memory (8) and saved on a computer disk as a bitmap file. The bitmap is an image data source for the "Textile Wettability Analyser" programme created in cooperation with the Department of Fibre Physics and Textile Metrology with the Computer Engineering Department of Technical University of Łódź. An algorithm for the analyser was created as a set of functions in a MATLAB 7 environment. The task of the analyser functions is to evaluate the contact angle by modelling the drop shape from the image acquired. All the measurements are carried out at a constant temperature of 24 $^{\circ}$ C.

■ Drop model assumptions

It is assumed that a drop of liquid is positioned on a horizontal textile surface in a state of balance resulting from the interaction between the force of vertical gravity and the interfacial tension force tangent to the liquid surface. In the image acquired the drop investigated can be seen as a dark profile with a clearly visible edge near apex A (Figure 2). The contact zone of the drop on the textile surface is visible as a grey strip of irregular width between a bright zone of air and the dark vertical cross-section of a textile specimen.

It is believed that the liquid drop forms contact angles less than 90 $^{\circ}$ to a textile background.

In the contact zone the following effects can be observed:

- 1) A reduction in the drop edge contrast compared with the contrast between liquid and air near the drop apex,
- 2) The change in the drop edge in its shadow edge, identified by the alteration of the edge direction. When the contact angles are less than 90 $^{\circ}$, the edge points of left and right semi-profiles increase their distances from the drop symmetry axis as they are further from the drop apex. Violation of this tendency means entering the shadow edge (in the vicinity of points P_1 , P_2 in Figure 2b).
- 3) The presence of the remains of a dark horizontal contact line which disappears as the distance grows between it and the three-phases contact points (P_1 , P_2) on some of the drop images acquired.

On the basis of the above-mentioned assumptions and observations, an algorithm for establishing a drop bottom line and for wetting (contact) angle evaluation is proposed.

■ Description of drop shape

A description of a drop shape is based on the axisymmetric drop shape analysis model - ADSA proposed by the Neumann group [7, 8]. Many variations of this model have been used (ADSA-P, ADSA-D) for sessile and pendant droplets to determine drop-air surface tension and wetting angles. The droplet edge can be described as a solution to the initial problem concerning the system of three ordinary differential equations of the first order versus the boundary parameter – [9, 11]:

$$\begin{aligned} dx/ds &= \cos(\phi), \quad dz/ds = \sin(\phi), \\ d\phi/ds &= 2 \times b - (\sin(\phi))/x - c \times z, \end{aligned} \quad (1)$$

where $b = 1/R_0$, $c = g \times \Delta\rho/\gamma$

Variables x , z , ϕ specify the abscissa, ordinate and polar angle of the tangent to (x, z) the trajectory point, where XZ is a right-handed coordinate system originating in the drop apex. Parameter b stands for drop surface curvature at the apex, c –capillary constant, g –gravity acceleration, γ – the interfacial tension between liquid and air, $\Delta\rho$ –the difference of liquid and air densities. The initial conditions are as follows:

$$x(0) = 0, \quad z(0) = 0, \quad \phi(0) = 0 \quad (2)$$

A set of differential equations (1) can be solved based on an explicit Runge-Kutta (4.5) formula using MATLAB function "ode45". The values of apex curvature b and capillary constant c should be determined before the beginning of calculations. The values are estimated on the basis of the features of the drop geometry and then optimised in the process of trajectory, fitting to the set of boundary data points. The numerical solution found has the form of a parametric trajectory curve $(x(s_j), z(s_j))$, $j \in [1, N]$, representing a drop profile boundary in the XZ coordinate system.

■ Image segmentation and analysis algorithm

Figure 3 (see page 86) show a flow diagram for the method proposed.

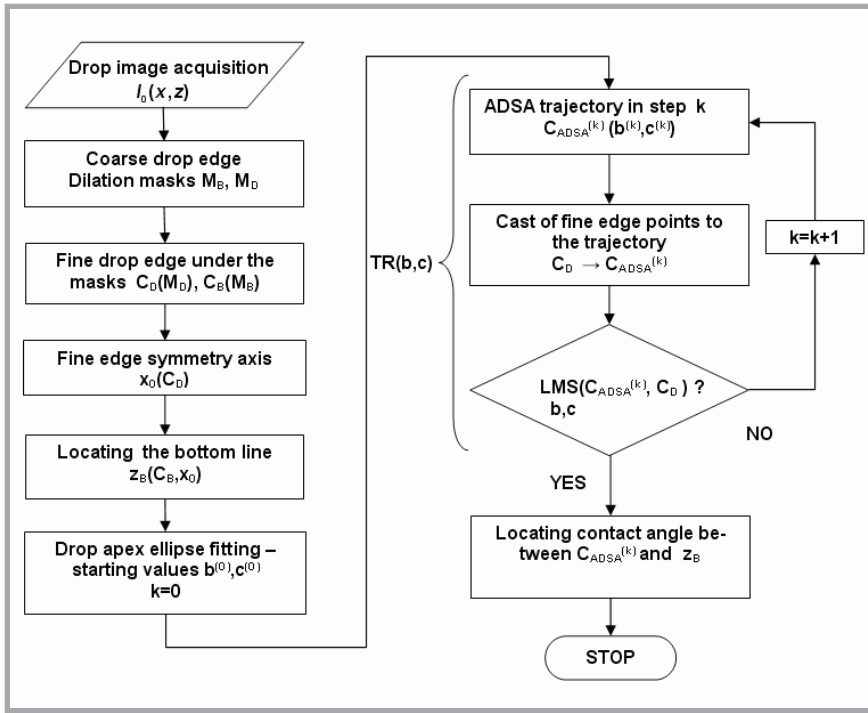


Figure 3. A flow diagram for the method proposed. M_B – dilation mask for baseline detection, M_D – the mask of droplet boundary points, b – the curvature in the drop apex, c – the capillary constant, $LMS(C_{ADSA}, C_D)$ – the least mean-square error of C_D data boundary approximation by ADSA trajectory, $TR(b,c)$ – the trust-region optimisation loop in b, c parameter space.

The algorithm proposed has the following steps:

- 1) Coarse drop contour detection using Canny filtering [14].

$$I_C(x, z) = Canny(I_0(x, z), T_1, T_2, \sigma) \quad (3)$$

Detection threshold T_2 , continuity threshold T_1 and standard deviation of the internal Gauss filter should be selected to detect the best contrasting upper part of the drop profile boundary above the contact zone. As a result a binary image $I_C(x, y)$ is obtained containing the base drop edge $C_{1,2}(x, z)$ (Figure 5.a).

- 2) Creation of ellipse $E_{LMS}(a_E, b_E, x_E, z_E)$ with centre (x_E, z_E) and $2a_E, 2b_E$ diameters best fitted, in least mean square (LMS) sense, to the $C_{1,2}(x, z)$ drop edge data. The algorithm of ellipse applied, which fitted the set of pixel data, was published in [13].

- 3) The setting of the masks for bottom line and drop boundary points. The E_{LMS} ellipse boundary is mapped into a binary image raster, and then two circular dilation masks [15, 16] are built around the pixels of this mapping. A symmetric, narrow mask M_D is used to limit source edge data for the ADSA

algorithm. An external mask M_B with a greater radius is applied to help with bottom line detection (Figure 2.b).

$$M_D = I(E_{LMS}) \oplus K(r_D), \quad (4)$$

$$M_B = M_D \oplus K(r_B)$$

- 4) The fine drop image boundary detection using Canny filtering. The parameters T_1, T_2, σ of the filter function (3) must be set to low values. Edge data points for bottom line detection and for the ADSA algorithm are selected under the M_B and M_D masks, respectively. Only the boundary objects with the greatest area AR for each mask type are taken into account. This way spurious edge fragments can be eliminated.

$$C_B(x, z) = \max_{AR} (I_C(x, z) \cap M_B) \quad (5)$$

$$C_D(x, z) = \max_{AR} (I_C(x, z) \cap M_D)$$

- 5) Evaluation of the horizontal coordinate x_0 of a vertical symmetry axis for the drop boundary C_D . For each row z , including edge points on the left and right sides of the apex $A(x_A, z_A)$ (Figure 2.b), their means $x_0(z)$ are evaluated, and then the global mean versus all z values.

$$x_0(z) = 1/2 \{ \text{mean}_x [x: (x, z) \in C_D, x \leq x_A] + \text{mean}_x [x: (x, z) \in C_D, x \geq x_A] \} \quad (6)$$

$$x_0 = \text{mean}_z \{ x_0(z) \} \quad (7)$$

- 6) Determination of the vertical coordinate z_B of the horizontal contact line by separately searching the location of points with the greatest distance to the symmetry axis x_0 for left and right drop semi-profiles.

$$z_B = \text{mean}_z (z), \quad (x, z) \in C_B, x = \max |x - x_0| \quad (8)$$

- 7) Boundary data symmetrisation versus the x_0 axis. It is based on evaluating the mean distance x from the edge data points (x, z) to the symmetry axis for each image row z .

- 8) Matching the numerical solution of drop boundary equations (1) – as sequence of trajectory points $(x(s_i), z(s_i))$ to the set of boundary data pixels $C_D = \{P_i(x_i, z_i)\}$ read from the drop image. It involves minimisation of the square distance between fine boundary data pixels and their orthogonal projections on the ADSA trajectory [9].

$$F(b, c) = \sum_i ((x_N(s_N, b, c) - x_i)^2 + (x_N(s_N, b, c) - x_i)^2) \quad (9)$$

where s_N – the trajectory parameter and the mean trajectory points $P_N(x_N, z_N)$ with the nearest Euclidean distance to appropriate data points (x_i, z_i) . Initial parameters for $F(b, c)$ optimisation are:

- a) Curvature $b = 1/R_0 = b_E/a^2_E$ at the drop apex calculated for the ellipse $E_A(a_E, b_E, x_E, z_E)$, matching, in least mean square sense, to drop boundary data near the apex. The curvilinear parameter s should not be greater than 1 - 2% of an estimated drop diameter.

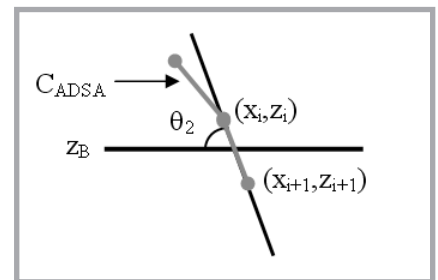


Figure 4. A picture explaining the method of contact (wetting) angle evaluation. C_{ADSA} – ADSA trajectory with points $(x_i, z_i), (x_{i+1}, z_{i+1}), \theta_2 = \theta$ – wetting angle (right).

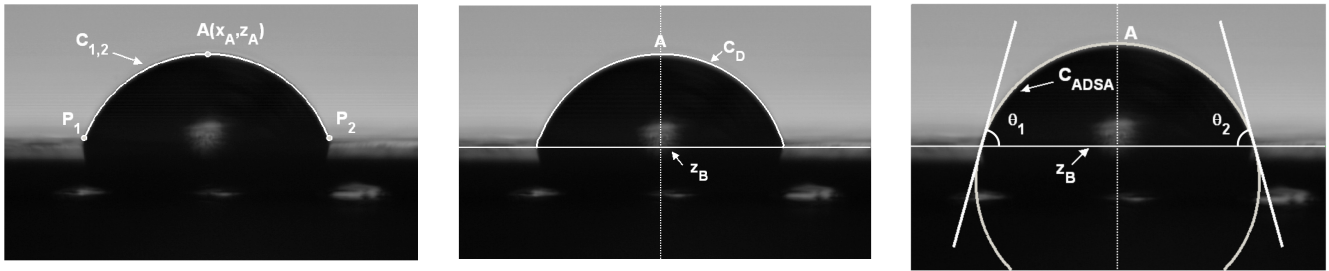


Figure 5. Selected stages of image processing and analysis for a sessile water droplet on a polyester textile surface: a) detection of the coarse drop edge $C_{1,2}$ using Canny filtering, b) detection of the fine drop edge C_D for the ADSA algorithm, c) the result of ADSA optimisation – C_{ADSA} trajectory and the contact angles $\theta_1 = \theta_2 = \theta$ measured at the intersection of C_{ADSA} with the bottom line z_B .

- b) Capillary constant c evaluated from equations (1) with the assumption that $x(z)$ is a function describing each half of the ellipse E_A :

$$z = b_E \left(1 - \sqrt{1 - x^2 / a_E^2} \right) \quad |x| \ll a_E \quad (10)$$

Functional (9) minimisation has been/is performed with the MATLAB function “lsqnonlin” using the large scale trust-region algorithm [17, 23] and error tolerance value “ToIX = 1e-6”. The path of trajectory points $(x(s), z(s))$ is defined as a polyline. In the case of $F(b, c)$ calculations are much faster when compared with the cubic spline interpolation of a trajectory curve. Adjusting the “MaxStep” option enables us to get a table of trajectory points dense enough to be linearly interpolated for data-trajectory distance measurements.

- 9) Evaluation of the liquid-textile contact angle θ as a polar angle of the line joining two neighbouring trajectory points $(x(s_i), z(s_i))$ and $(x(s_{i+1}), z(s_{i+1}))$. The distance between these points must be intersected by the horizontal contact line z_B (Figure 4).

Examples and experimental results

Figure 5 presents the main algorithm steps for a sessile water drop on a horizontal polyester textile surface. The canny filter parameters for coarse edge detection $C_{1,2}$ (Figure 5.a) are $T_2 = 0.9, T_1 = 0.7, \sigma = 3$ and for fine edge detection $T_1 = 0.1, T_2 = 0.2, \sigma = 1$ (Figure 5.b). The algorithm has relatively low sensitivity to T_1, T_2, σ Canny filter parameters, so they do not need to be changed in the whole series of drop images acquired

In Figure 5.c the final ADSA curve (C_{ADSA}) is visible after optimisation in parameter space TR(b, c) (Figure 3).

Contact (wetting) angles $\theta_1 = \theta_2 = \theta$ at the intersection points of C_{ADSA} with the bottom line z_B are visible as well.

A series of contact angle measurements has been/were carried out for water droplets on a polyester textile background applying both computer and manual methods (Table 1). In the manual image method both the bottom line and elliptic shape are manually fitted to the drop profile [24]. Wetting angles are measured between the bottom line and the automatically calculated ellipse tangents.

Measurement results for the two methods are compared in Table 1, based on the same set of images. Normal distributions are assumed, and X, Y measurement results for the same drop objects correlated. The average value of the difference random variable $Z = X - Y$ has student’s distribution [18]:

$$st = \frac{\text{average}(Z)}{S_Z} \sqrt{n-1} \quad (11)$$

where Z – a random variable of the measurement differences, S_Z – standard deviation of Z, n – the number of measurements.

In the case of the data in Table 1:

$$st = \frac{2.44}{2.40} \sqrt{10-1} \approx 3.05 \in R_{0.05}$$

$$R_{0.05} = (-\infty, -2.26) \cup (2.26, \infty)$$

with $R_{0.05}$ – a double sided critical region of significance level equal to 0.05.

The above student’s t-test gives the result of $3.05 > 2.26$ –critical region limit at a significance level of 0.05. For the two measurement methods shown in Table 1, the hypothesis of equal average results at a significance level of 0.05 must be rejected. This result can be easily explained. In the manual method the ellipse is fitted to the pixels of a drop edge intersection with a bottom line. In this case the height of the ellipse segment is slightly lower than the drop apex, as well as the angles of the ellipse tangents. The standard deviations calculated for both methods are greater than shown in literature examples [8] for smooth backgrounds, because the surfaces of textiles are usually non-uniform. For them only average values of contact angles for a series of measurements make sense.

Table 1. Contact angles evaluated by computer and manual methods for water drops on polyester textile surfaces.

No.	Contact angles evaluated, °		Difference, ° (Z = X - Y)
	Computer version (X)	Manual version (Y)	
1	71.70	73.06	-1.36
2	73.64	70.63	3.01
3	71.74	68.27	3.47
4	74.36	66.47	7.89
5	74.34	70.81	3.53
6	77.07	75.14	1.93
7	76.65	73.39	3.26
8	73.74	71.65	2.09
9	68.63	69.84	-0.21
10	68.71	67.91	0.80
average	73.15	70.71	2.44
S.D.	2.73	2.70	2.40

■ Conclusions

The suggested method of contact angle measurement is applied to flat textile specimens and to angles less than 90°, when the bottom line cannot be determined without ambiguity. The method is based on the ADSA model, taking into account actions of the force of gravity and interfacial tension, expressed by Equations (1). Owing to this it is possible to evaluate the proper shape of a drop profile under examination, whereas for ellipse fitting this can only be done on the basis of its geometrical similarity to the shape of a drop profile. Moreover, the process of interactive fitting suffers from subjective human error. The use of the sessile drop technique provides better simulation of natural textile wetting conditions than the Wilhelmy or wicking methods [5, 6]. The method presented requires a selection of textile surfaces and illumination conditions to enable visibility of the residual contact line or drop shadow boundaries.



References

1. M. Żenkiewicz, "Adhesion and modification of polymer surface", WNT, Warszawa 2000.
2. S. Siboni, C. Della Volpe, D. Maniglio, M. Brugnara, "The solid surface free energy calculation, part I and II", *J. Colloid and Interface Sci.* 271, 2004, pp. 454-472.
3. L.-J. Dogue, N. Mermilliod, G. Boiron, S. Steveris, "Improvement of polypropylene film adhesion in multilayers by various chemical surface modifications", *Int. J. Adhesion and Adhesives* 1995, (15), pp. 205-210.
4. G. Cantero, A. Arbelaz, R. Llano-Ponte, I. Mondragon, "Effects of fibre treatment on wettability and mechanical behaviour of flax / polypropylene composites", *Composites Science and Technology* 2003, (63), pp. 1247-1254.
5. Yongan Gu, "Contact angle measurement techniques for determination of wettability", *Encyclopedia of surface and colloid science*, ed. Marcel Dekker, 2002, pp. 1213-1227.
6. M. Espinosa-Jimenez, A. Ontiveros-Ortega, R. Perea-Carpio, E. Gimenez-Martin "Interfacial chemistry of fabric surfaces", *Encyclopedia of surface and colloid science*, ed. Marcel Dekker, 2002, pp. 2784-2786.
7. S. Lahooti, O. I. del Rio, A. W. Neumann, P. Cheng, "Axisymmetric drop shape analysis (ADSA)", A.W. Neumann, J.K. Spelt (Eds.) *Applied Surface Thermodynamics*, Marcel Dekker, New York, 1996, p. 379.
8. J. M. Alvarez, A. Amirfazli, A. W. Neumann, "Automation of the axisymmetric drop shape analysis-diameter for contact angle measurements", *Colloids and Surfaces, A: Physicochem. and Eng. Aspects* 156, 1999, pp.167-176
9. I. T. Concept, "Drop Tensiometer", www.itconceptfr.com/BrochureTracker/Documentation_Tracker_.htm.
10. FIBRO System AB, "PGX-Goniometer", www.klimatest.com/v01/Contact_Angle.
11. A. Konno, K. Izumiyama, "On the oil/water interfacial tension and the spread of oil slick under ice cover", *The 17th International Symposium on Okhotsk Sea & Sea Ice* (2002), pp. 275-282.
12. A. Konno, K. Izumiyama. "Theory and modeling of the interfacial tension force on the oil spreading under ice covers", *Proceedings of the 16th IAHR International Symposium on Ice, Dunedin, New Zealand, 2nd-6th December 2002*, pp. 185-192.
13. A. Fitzgibbon, M. Pilu, R. B. Fisher "Direct Least Square Fitting of Ellipses", *PAMI*, Vol. 21, No. 5, May 1999, pp. 476-480.
14. J. F. Canny, "A computational approach to edge detection", *IEEE Trans. Pattern Analysis and Machine Intelligence*, Nov 1986, 8(6), pp. 679-698
15. J. Serra, "Introduction to Mathematical Morphology", *Computer Vision, Graphics and Image Processing*, Vol. 35 1986, pp. 283-305.
16. W. Malina, M Smiatacz, "Metody cyfrowego przetwarzania obrazów", EXIT, Warszawa 2005
17. "The Mathworks Optimization Toolbox", <http://www.mathworks.com/helpdesk/help/toolbox/optim>
18. D. Bobrowski, "Probabilistyka w zastosowaniach technicznych", WNT, Warszawa 1980
19. R. M. Haralick, L. G. Shapiro, "Computer and Robot Vision", Vol. I, Addison-Wesley, 1992, pp. 158-205.
20. van den Boomgaard, van Balen, "Image Transforms Using Bitmapped Binary Images", *Computer Vision, Graphics, and Image Processing: Graphical Models and Image Processing*, Vol. 54, No. 3, May, 1992, pp. 254-258.
21. J. E. Dennis, "Nonlinear Least Squares, State of the Art in Numerical Analysis", ed. D. Jacobs, Academic Press, 1977, pp. 269-312.
22. T. F. Coleman, Y. Li, "On the Convergence of Reflective Newton Methods for Large-Scale Nonlinear Minimization Subject to Bounds", *Mathematical Programming*, Vol. 67, Number 2, 1994, pp. 189-224.
23. T. F. Coleman, Y. Li, "An Interior, Trust Region Approach for Nonlinear Minimization Subject to Bounds", *SIAM Journal on Optimization*, Vol. 6, 1996, pp. 418-445.
24. S. Sosnowski, W. Urbaniak-Domagala, unpublished works of "Department of Fibre Physics and Textile Metrology"



Received 15.01.2007

Reviewed 23.04.2007

3rd INTERNATIONAL CONFERENCE "SMART MATERIALS, STRUCTURES AND SYSTEMS"

June 8-13, 2008 Acireale,
Sicily, Italy

Including well over 700 scientific and technical contributions, the Conference will provide an interdisciplinary forum for the exchange of the latest information and ideas in this rapidly advancing research area.

Technical sessions will span the most recent leading developments in smart materials and microsystems, smart and adaptive optics, intelligent autonomous structures, DNA technologies, biomedical applications, bioinspired materials and bionic systems.

The following Symposiums are to be featured:

- A - SMART MATERIALS AND MICRO & NANOSYSTEMS
- B - SMART OPTICS
- C - SMART STRUCTURES AND INTEGRATED SYSTEMS
- D - BIOMEDICAL APPLICATIONS OF SMART MATERIALS, NANOTECHNOLOGY AND MICRO/NANO ENGINEERING
- E - MINING SMARTNESS FROM NATURE

And the following

Focused / Special Sessions:

- Recent Development in Electrical Writable Organic Memory Devices
- State-of-the-art Research and Application of SMAs Technologies
- Smart Textiles
- Artificial Muscle Actuators using Electroactive Polymers
- Biomimetic Flow Control in Aquatic Systems and its Application to Bioinspired Autonomous Underwater Vehicles

Contact:

CIMTEC 2008
Ms Stefania Bianchedi
P.O. Box 174, 48018 FAENZA-ITALY
Phone + 0546 22461 Fax + 0546 664138
Email: congress@technanogroup.it